Journal of Organometallic Chemistry, 427 (1992) 369–378
Elsevier Sequoia S.A., Lausanne
JOM 22436

Synthesis, crystal structure and spectroelectrochemistry of $[(C_5Me_5Ru)_2\text{-}\eta^6,\eta^6\text{-chrysene}]^{2+}(O_3SCF_3^-)_2$. Formation of $[(C_5Me_5Ru^I)(C_5Me_5Ru^{II})\text{-}\eta^6,\eta^6\text{-chrysene}]O_3SCF_3$

Ivonne Chavez, Margarita Otero, Enrique Román *
Facultad de Química, Pontificia Universidad Católica de Chile, Casilla 306, Correo 22, Santiago (Chile)

and Ulrich Müller
Fachbereich Chemie der Universität, Hans-Meerwein-Straße, W-3550 Marburg (Germany)

(Received July 20, 1991)

Abstract

The binuclear complex $[(C_5Me_5Ru)_2\text{-}\eta^6,\eta^6\text{-chrysene}](O_3SCF_3)_2$ (**1**) was synthesized from $[C_5Me_5Ru(CH_3CN)_3]O_3SCF_3$ and chrysene in THF. Complex **1** is reduced by sodium naphthalene to the mixed valence complex $[(C_5Me_5Ru^I)(C_5Me_5Ru^{II})\text{-}\eta^6,\eta^6\text{-chrysene}]O_3SCF_3$ (**2**), which is thermodynamically stable (coproportionation constant $K_c = 2.57 \times 10^5$). Complex **2** is also formed by electrochemical reduction, as established by cyclovoltammetry and coulometry; the reduction $\mathbf{1}^{++} + e \leftrightarrows \mathbf{2}^{+\cdot}$ is reversible with $E_1 = -1.37$ V (*vs.* saturated calomel electrode), and at $E_2 = -1.69$ V a second, irreversible reduction takes place. In ESR at 140 K, **2** shows $g_1 = 2.025$, $g_2 = 2.009$ and $g_3 = 1.998$ ($g_{iso} = 2.011$). An intervalence absorption band is observed for **2** in the visible–near IR spectrum. ^1H-NMR and ^{13}C-NMR data are reported for **1**. A dielectronic reduction of $\mathbf{1}^{++}$ with two equivalents of sodium naphthalene affords the unstable diamagnetic and neutral $[(C_5Me_5)_2Ru_2\text{-}\eta^5,\eta^5\text{-chrysene}]$ (**3**) that probably has a cyclohexadienyl configuration configuration respect to the Ru^{II}-chrysene bonds. An X-ray crystal structure determination was performed for **1**. In the centrosymmetric doubly charged cation in **1** each of the two Ru atoms has a sandwich-type coordination between a C_5Me_5 group and one of the terminal chrysene rings.

Introduction

In continuation of our studies on the syntheses, structures and electrochemistry of binuclear sandwich complexes of ruthenium(II) containing polycondensed aromatic ligands [1], we present results on the thermodynamic stability of an mixed valence Ru^IRu^{II} compound. Much knowledge about electrochemical and structural properties of mixed-valency complexes $M^{III}M^{II}$, $M^{II}M^I$, and M^IM^0 has

---

Correspondence to: Professor E. Román, Centro de Investigación Minera y Metalúrgica, Las Condes, Casilla 170, Correo 10, Santiago, Chile or Professor U. Müller, Fachbereich Chemie der Universität, Hans-Meerwein-Straße, W-3550 Marburg, Germany.

already been gathered [2], that which concerns $Fe^{II}Fe^{I}$ compounds with polyaromatic ligands [3] being the most closely related to our work. Some information was published recently for binuclear complexes containing $[Cp^*Ru^{II}]^+$units [4]. In this paper we present a complete description of the electron transfer properties and the structure of the binuclear cation $[(Cp^*Ru)_2\text{-}\eta^6,\eta^6\text{-chrysene}]^{2+}$, which relates it to materials having electrochromic properties and conductivity in the solid state [5].

Results and discussion

Synthesis

Attachment of the fragment $[Cp^*Fe]^+$ to a polyaromatic ligand requires drastic reaction conditions (high temperature, presence of excess $AlCl_3$), which limits its use in synthesis to thermostable systems [3,6]. In contrast, $[Cp^*Ru]^+$ fragments bind to orthocondensed polyaromatics under mild conditions [4]. We decided to use Fagan's approach [4a], and devised a high-yield, high-selectivity route involving the following reactions:

$$\tfrac{1}{4}[Cp^*RuCl]_4 + AgO_3SCF_3 + 3MeCN \xrightarrow[\text{r.t.}]{\text{MeCN}} [Cp^*Ru(NCMe)_3]O_3SCF_3 + AgCl$$

$$n[Cp^*Ru(NCMe)_3]O_3SCF_3 + \text{polyarene} \xrightarrow[\text{r.t.}]{} [(Cp^*Ru)_n\text{polyarene}]^{n+} + 3n\text{MeCN} + nCF_3SO_3^-$$

$n = 1, 2, 3, \ldots$

We describe here the compound $[(Cp^*Ru)_2\text{-}\eta^6,\eta^6\text{-chrysene}](O_3SCF_3)_2$ (**1**) which is formed with 93% yield. Dissociation of this complex by the action of solvents,

$$[(Cp^*Ru)_2\text{chrysene}]X_2 + 6\text{Solv} \rightarrow 2[Cp^*Ru\ \text{Solv}_3]^+ + \text{chrysene} + 2X^-$$

$\mathbf{1}$: $X^- = F_3CSO_3^-$ $\quad$ $X = PF_6^-, F_3CSO_3^-$

$\mathbf{1}^{++}$: cation $\quad$ Solv = THF, MeCN, acetone

is rather slow (not detectable in several hours) in acetonitrile or acetone, probably because of the higher thermodynamic stability of the ion-pair $[(\mathbf{1})\ (O_3SCF_3)_2]$ compared with that of hexafluorophosphate salts [7]. In this case, a rapid coordination of the $[Cp^*Ru]^+$ group is observed. The double coordination of $[Cp^*Ru^+]$ to the chrysene framework shows a selectivity towards the terminal rings, and ring bonding isomers are not observed.

The yellow salt **1** can be reduced with sodium naphthalene to yield dark blue-violet, paramagnetic $[(Cp^*Ru^I)(Cp^*Ru^{II})\text{chrysene}]^+[O_3SCF_3]^-$ (**2**), which is extremely sensitive towards oxygen.

Crystal structure of $[(Cp^*Ru)_2chrysene](O_3SCF_3)_2$, 1

Crystal data for **1** and details of the X-ray structure determination are given in Table 1 and the atomic parameters in Table 2.

The $F_3CSO_3^-$ ions in complex **1** showed high thermal motion or disorder and this caused problems during the refinement and prevented attainment of a lower *R* index. The cations have the structure shown in Fig. 1. They are centrosymmetric about an inversion centre between atoms C(19) and C(19′). The Cp* ligands,

Table 1

Crystal data and details for the X-ray structure analysis of **1** [a]

Lattice parameters	$a = 1308.7(2)$, $b = 1634.6(3)$, $c = 1937.6(4)$ pm $V = 4145(1) \times 10^{-30}$ m^3
Z	4
Density (calculated)	1.60 g cm^{-3}
Space group	*Pbca*
Diffractometer	4-circle, Enraf-Nonius CAD4
Radiation	Mo-K_α (graphite monochromator), $\lambda = 71.07$ pm
Temperature	20°C
Lattice parameter calculation	15 reflections, $15° < \theta < 21°$
Range measured	$1.5° < \theta < 21°$
Scan type	ω-scan, $\Delta\omega = 0.80 + 0.35 \tan \theta°$
Number of measured reflections	2825
Number of unique reflections	2240; $R_{\text{int}} = 0.016$
Unobserved reflections ($F < 3\sigma(F)$)	847
Corrections	Lorentz and polarisation factor, absorption
Linear absorption coefficient	$\mu = 8.1$ cm^{-1}
Transmission factors	0.74 to 0.94
Structure determination	Patterson synthesis
Refinement	Minimization of $\Sigma w(\lvert F_o \rvert - \lvert F_c \rvert)^2$, $w = 1/\sigma^2(F)$
Comments	High anisotropic temperature factors for the Cp* ring and especially for the $F_3CSO_3^-$ ion and improbable C–F bond lengths suggest some disorder
Programs used	[13,14]
Atomic form factors, f', f''	[15]
$R = \Sigma \lVert F_o \rvert - \lvert F_c \rVert / \Sigma \lvert F_o \rvert$	0.088
$wR = [\Sigma w(\lvert F_o \rvert - \lvert F_c \rvert)^2 / \Sigma w F_o^2]^{1/2}$	0.043

[a] Tables of anisotropic thermal parameters and structure factors have been deposited. Copies may be obtained from the Fachinformationszentrum Karlsruhe, W-7514 Eggenstein-Leopoldshafen 2, Germany, stating the authors, journal and depository number CSD-55877.

especially their methyl groups, also show high thermal motion in the sense of vibrations of the rings about axes perpendicular to the ring centres.

The bond distances (Table 3) agree with those found for the mononuclear complex [(Cp*Ru)-η^6-chrysene]PF$_6$ [1], the mean values being 221 pm for the Ru–C(Cp*) and 223 pm for the Ru–C(chrysene) bonds. In both compounds one Ru–C(chrysene) bond (Ru–C(16)) is longer than the others. As in other Cp*Ru arene complexes, such as [Cp*Ru(C$_6$Me$_6$)]* [4a], the aromatic rings are parallel to one another.

Spectrochemical characterization

^{1}H-NMR and ^{13}C-NMR data for **1** are summarized in Table 4. The assignments relate to the numbering scheme used in Fig. 1. The protons H(17) and H(18) of the uncomplexed rings show up as two doublets, at $\delta = 7.82$ and 8.75 ppm, assignable to an AB coupling system with a coupling constant of $^3J = 9.33$ Hz. Two further doublets ($\delta = 6.53$ and 7.62 ppm) are assigned to H(11) and H(14), respectively: they are coupled with the other H-atoms of the complexed rings of the chrysene H(12) and H(13), respectively, which show up as two pseudotriplets centred at $\delta = 6.23$ and 6.07 ppm. They show shielding induced by the complexation to the

Table 2

Atomic coordinates and parameters $U(\text{Å}^2)$ for the equivalent anisotropic [16] temperature factor $\exp(-8\pi^2 U \sin^2\theta/\lambda^2)$

Atom	*x*	*y*	*z*	*U*
Ru	0.2477(2)	0.0465(1)	0.07774(8)	0.0414(4)
C(1)	0.192(2)	0.172(2)	0.065(2)	0.08(2)
C(2)	0.306(2)	0.176(2)	0.083(2)	0.05(1)
C(3)	0.315(2)	0.134(1)	0.155(1)	0.05(1)
C(4)	0.208(2)	0.105(2)	0.175(1)	0.06(1)
C(5)	0.137(2)	0.132(2)	0.121(1)	0.08(1)
C(6)	0.154(2)	0.218(1)	−0.002(1)	0.10(1)
C(7)	0.393(2)	0.209(1)	0.045(1)	0.08(1)
C(8)	0.407(2)	0.121(1)	0.195(1)	0.08(1)
C(9)	0.181(2)	0.067(1)	0.240(1)	0.09(1)
C(10)	0.022(1)	0.126(1)	0.121(1)	0.08(1)
C(11)	0.201(2)	−0.024(1)	−0.015(1)	0.034(9)
C(12)	0.153(2)	−0.057(2)	0.042(1)	0.05(1)
C(13)	0.218(1)	−0.086(1)	0.101(1)	0.034(9)
C(14)	0.331(2)	−0.068(1)	0.094(1)	0.05(1)
C(15)	0.372(2)	−0.032(2)	0.037(1)	0.06(1)
C(16)	0.308(2)	−0.009(2)	−0.025(2)	0.05(1)
C(17)	0.345(2)	0.027(1)	−0.084(1)	0.044(8)
C(18)	0.449(2)	0.041(1)	−0.087(1)	0.046(8)
C(19)	0.519(2)	0.019(1)	−0.028(1)	0.05(1)
S	0.5582(6)	0.1167(5)	0.6942(4)	0.068(3)
F(1)	0.666(3)	0.246(2)	0.663(1)	0.28(2)
F(2)	0.650(2)	0.222(1)	0.7688(9)	0.19(1)
F(3)	0.737(2)	0.154(1)	0.711(2)	0.24(2)
O(1)	0.551(2)	0.069(1)	0.751(1)	0.19(1)
O(2)	0.478(2)	0.164(1)	0.684(1)	0.23(2)
O(3)	0.588(2)	0.079(1)	0.633(1)	0.21(1)
C	0.647(3)	0.197(4)	0.707(2)	0.14(2)

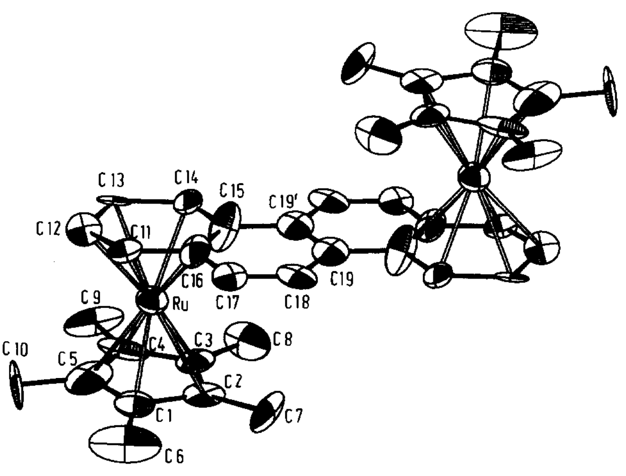

Fig. 1. Structure of the $[(C_5Me_5Ru)_2\text{-}\eta^6,\eta^6\text{-chrysene}]^{++}$ ion with ellipsoids of thermal motion (50% probability; H atoms omitted).

Table 3

Bond lengths (pm) in $[(C_5Me_5Ru)_2$-η^6,η^6-chrysene$](O_3SCF_3)_2$

Ru–C(1)	220(3)	Ru–C(11)	222(2)
Ru–C(2)	224(3)	Ru–C(12)	221(2)
Ru–C(3)	225(2)	Ru–C(13)	224(2)
Ru–C(4)	216(3)	Ru–C(14)	219(2)
Ru–C(5)	218(2)	Ru–C(15)	221(3)
C(1)–C(2)	153(3)	Ru–C(16)	232(3)
C(2)–C(3)	156(3)	C(11)–C(12)	138(3)
C(3)–C(4)	151(3)	C(12)–C(13)	149(3)
C(4)–C(5)	146(3)	C(13)–C(14)	151(2)
C(5)–C(1)	146(4)	C(14)–C(15)	136(3)
C(1)–C(6)	157(3)	C(15)–C(16)	150(3)
C(2)–C(7)	146(3)	C(15)–C(19′)	145(3)
C(3)–C(8)	146(3)	C(16)–C(11)	143(3)
C(4)–C(9)	145(3)	C(16)–C(17)	137(3)
C(5)–C(10)	150(3)	C(17)–C(18)	138(2)
		C(18)–C(19)	150(3)
S–C	177(4)	C(19)–C(19′)	134(3)
S–O(1)	135(2)	C–F(1)	118(6)
S–O(2)	133(2)	C–F(2)	126(5)
S–O(3)	138(2)	C–F(3)	138(5)

$[Cp^*Ru^+]$ fragments. For the methyl protons of the η^5-C_5Me_5 groups only a single peak is observed, and this arises from the above-mentioned large thermal motion. In the decoupled ^{13}C-NMR spectra **1** shows a quartet at 126.25 ppm for the $F_3CSO_3^-$ ion (due to coupling with the ^{19}F nuclei), a single peak for the methyl groups of the Cp* rings at 9.92 ppm, and two groups of peaks due to the chrysene. One group with $\delta = 128.71$ and 126.25 ppm corresponds to the atoms C(17) and C(18) of the uncomplexed rings, while the other group with δ values between 82 and 96 ppm can be assigned to the atoms of the complexed rings of the chrysene. Peaks due to the quaternary C atoms cannot be clearly seen in the spectrum.

Table 4

^{1}H- and ^{13}C{H}-NMR data [a] for $[(C_5Me_5Ru)_2$-η^6,η^6-chrysene$](O_3SCF_3)_2$

^{1}H(300 MHz) [b]	^{13}C{H}[c] (75.4 MHz)
8.75 (d; 2H; AB; $^3J = 9.33$ Hz); H(18)	128.71 (uncomplexed-C ring)
7.82 (d; 2H; AB; $^3J = 9.33$ Hz); H(17)	126.25 (uncomplexed-C ring)
7.62 (d; 2H; $^3J = 6.29$ Hz); H(14)	122.32 (q, O_3SCF_3)
6.53 (d; 2H; $^3J = 5.88$ Hz); H(11)	95.87 (complexed-C ring)
6.23 (pt; 2H; AA′BB′; $^3J = 6.29$; $^3J = 5.80$ Hz); H(13)	88.91 (complexed-C ring)
6.07 (pt; 2H; AA′BB′; $^3J = 5.84$; $^3J = 5.83$ Hz); H(12)	86.50 (complexed-C ring)
1.57 (s; 30 H); (Me-Cp*)	82.35 (complexed-C ring)
	9.92 (Me-Cp*)

[a] ppm *vs.* tetramethylsilane at 25°C in CD_2Cl_2 (s = singlet; d = doublet; pt = pseudotriplet; q = quartet). [b] Numbering of the H atoms corresponds to the numbering of the C atoms in Fig. 1. [c] Proton decoupled; quaternary carbon atoms were not assigned.

Table 5

UV spectra and ESR g values of [(Cp*Ru)$_n$-chrysene]X$_n$; $n = 1, 2$; X = CF$_3$SO$_3^-$, PF$_6^-$

Compound	g factors [a]	λ_{max} [b] (ϵ (dm^3 mol^{-1} cm^{-1}))
1	–	334 (12.152)
		392 (3.189)
		416 (2.850) (sh)
2	$g_{iso} = 2.0111$	392
	$g_1 = 2.0256$	518 (sh)
	$g_2 = 2.0095$	562
	$g_3 = 1.9989$	600–830 [c]
[(Cp*Ru)-chrysene)(PF$_6$) [d]	–	328 (5.483)
		360 (2.973)

[a] At 140 K in propylene carbonate. [b] In acetone; sh = shoulder. [c] Broad low energy band (IVB). [d] See ref. 1.

The UV-visible spectral data for **1** and **2** and ESR values for **2** are given in Table 5. Compared with those for [(Cp*Ru)chrysene]O$_3$SCF$_3$ and other mononuclear Cp*Ru-polyarene complexes [1,7], the data for **1** show a bathochromic shift. In acetone solution there is a ligand field peak ($\lambda = 392$ nm, $\epsilon = 3.189$ dm^{3}mol^{-1}cm^{-1}) with a shoulder ($\lambda = 416$ nm); this band is solvent-dependent and corresponds to the $^1A_1 \rightarrow {}^1E_1$ (d–d) electronic transition with an important metal–ligand orbital contribution, as suggested for analogous metallocene-d^6 complexes [7]. Furthermore, an intense, solvent-independent band, with a characteristic fine structure due to the $\pi \rightarrow \pi^*$ intraligand electronic transition, appears at $\lambda = 334$ nm ($\epsilon = 12.152$). The spectrum of **2** is discussed below.

Spectroelectrochemistry

The binuclear cation $\mathbf{1}^{++}$, having 36 valence electrons (counting only complexed π and metal-d electrons), undergoes electrochemical reduction in two independent steps (Fig. 2) with an energy difference of $\Delta E = 320$ mV between the monoelectronic steps (Table 6).

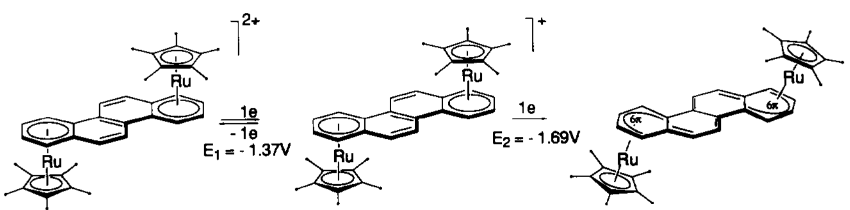

$\mathbf{1}^{++}$ $\mathbf{2}^{+\cdot}$ **3**

The disproportionation potential for the monocation $\mathbf{2}^{+\cdot}$ is thus -0.32 V and the conproportionation constant for the mixed valence species [Ru^{I}–Ru^{II}]$^+$ is $K_c = 2.57 \cdot 10^5$. Diffusion-controlled electron transfer was established for the first wave (ipc/$v^{1/2}$ is constant over a wide range; Fig. 2). Electrochemical and chemical reversibility was confirmed for the first wave by the peak separation ($\Delta E_p = 50$ to 100 mV and ipa/ipc = 1); in the case of the ferrocene/ferricinium couple a similarly large peak separation under the same conditions was used as criterion for reversibility [10]. The second wave corresponds to an electrochemically and chemically irreversible electron transfer process, $\mathbf{2}^{+\cdot} + e \rightarrow \mathbf{3}$. The mono-

Table 6

Peak and mean potentials [a] of cationic [(Cp*Ru)$_n$-chrysene]X$_n$, $n = 1, 2$; X = $CF_3SO_3^-$, PF_6^-

Compound		$-E_{pc}$ (V)	ΔE_p (mV)	ia/ic	n	Characteristics
1	first wave [b]	1.37	60	1	1	reversible $\mathbf{1}^{++} + 1\,e \rightleftarrows \mathbf{2}^{+}$
	second wave [b]	1.69	–	–	–	irreversible $\mathbf{2}^{+} + 1e \rightarrow \mathbf{3}$
[(Cp*Ru)-chrysene)PF$_6$ [c]		1.72	210	0.55	1	irreversible

[a] Propylene carbonate, NEt_4ClO_4, 0.1 mol/l; 20°C on GCE. [b] v = 50 to 700 mV/s. [c] see ref. 1.

cationic, dark blue-violet 37 electron species $\mathbf{2}^{+\cdot}$ was also generated by electrochemical reduction of **1** by electrolysis at a controlled potential on a platinum electrode ($E_{work} = -1.40$ V, *vs.* saturated calomel electrode, SCE) in propylene carbonate, NEt_4ClO_4 0.1 mol/l). The UV–visible absorption spectrum changes in the course of the electrolysis (Fig. 3), showing the formation of a stable species possessing a broad low energy intervalence band, in the near infrared ($\lambda > 830$ nm) and two more bands ($\pi \rightarrow \pi^*$ at $\lambda = 334$ nm; ligand-field band at 563 nm). The kinetic data for this one-electron reduction of $\mathbf{1}^{++}$ reveal it to be a first-order process with $k_{ET} = 9.37 \times 10^{-3}$ s^{-1}, as shown by the increasing intensity of the band at 392 nm and the appearance of the band at 563 nm. This further supports the presence of the mixed valence [Ru^{I}–Ru^{II}] species in $\mathbf{2}^{+\cdot}$.

The species $\mathbf{2}^{+\cdot}$, electrochemically generated in the cavity of the ESR spectrometer at 140 K shows an orthorhombic paramagnetic behaviour with the following g values: g_1, 2.025; g_2, 2.009; g_3, 1.998 ($g_{iso} = 2.011$). Satellite bands due to ^{109}Ru

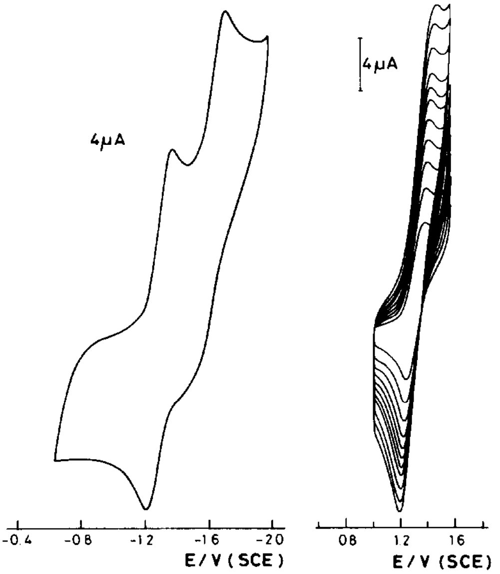

Fig. 2. Cyclic voltammograms of **1** (5×10^{-3} mol/l in propylene carbonate). Left: v = 200 mV/s. Right: on a glassy carbon electrode in propylene carbonate; scan rates from 50 to 700 mV/s.

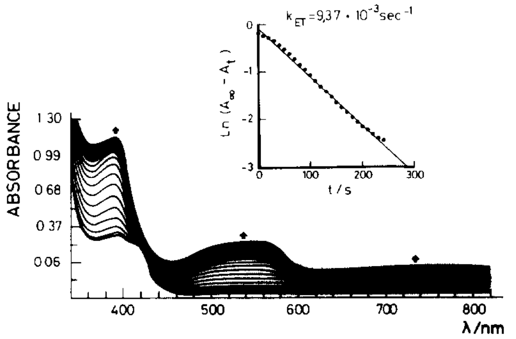

Fig. 3. Spectrochemical changes during controlled potential electrolysis at $E_1 = -1.40$ V (SCE) of **1** (5×10^{-3} mol/l) in propylene carbonate. The inset plot shows the linearity for the increase of the $\lambda = 392$ nm absorption.

($S = 5/2$) are also observed, showing significant interaction of the radical electron with the metal atoms [8].

In contrast to the cation $\mathbf{1}^{++}$, the mononuclear complex [(Cp*Ru)chrysene]PF_6 [1] shows only one irreversible reduction with a more negative potential ($E = -1.27$ V (SCE)); this is the case for other similar compounds [4c]. The thermodynamic stability of $\mathbf{2}^{+\cdot}$ must therefore involve a higher degree of delocalization, with considerable contribution of the LUMO-e_1* orbitals of the Ru atoms. After the complete reduction to **3** no paramagnetic signal was observable, suggesting a cyclohexadienyl mode of binding for the end rings of the chrysene component, as formulated in the above formula scheme; this has been shown to be the case for dielectric reductions of binuclear [$(arene)_2Ru$]$^{++}$ complexes [9]. Finally, the NMR properties at the neutral complex **3** show it to be diamagnetic, but we were not able to isolate it.

Experimental

All reactions were performed under an atmosphere of dry argon by use of Schlenk techniques and a dry box. Solvents were dried and distilled prior to use. [Cp*$RuCl$]$_4$ and [Cp*$Ru(CH_3CN)_3$]O_3SCF_3 were prepared from $RuCl_3 \cdot xH_2O$ (Aldrich) as previously described [4a]. Chrysene was of commercial grade (Aldrich). Sodium naphthalene was prepared in THF from naphthalene and sodium, and the concentration in the resulting green solution was determined by titration with HCl(aq). ^{1}H-NMR spectra (300 MHz) and ^{13}C-NMR (75.4 MHz) were recorded with a Bruker 300 spectrometer. Cyclovoltammetry and coulometry were performed with a Wenking HP-72 potentiostat, triangular signal generator Wenking VSG-72; propylene carbonate, NEt_4ClO_4 0.1 mol/l, SCE as reference, Ru complex $5 \cdot 10^{-3}$ mol/l; ferrocene was introduced as internal reference at the end of each measurement ($E° = +0.4$ V [10]). A digital integrator Wenking EVI-80 was included in the circuit for coulometry during electrolyses with Pt as working electrode (up to 10% of the theoretical quantity). Spectroelectrochemical measurements were performed with the P-72 potentiostat and a Hewlett-Packard 8452A photodiode array spectrophotometer with a gold minigrid (100 wires in^{-1}, 80% transmittance) as working electrode; cell design as in [11]. The pseudo first order heterogenous electron transfer constant was taken from the slope of $\ln(A_t - A_\infty)$ *vs.* A_∞ plot (A_∞, A_t = absorbance at equilibrium and at time t, respectively). ESR measurements were performed at various temperatures with an electrochemical cell mounted inside the cavity of a Bruker ER-10 spectrometer, the equipment was as previously reported [8,12].

Bis-(η^5-pentamethylcyclopentadienyl-ruthenium)-η^6,η^6-chrysenium bis-trifluoromethanesulfonate, 1. A solution of 100 mg of chrysene (0.438 mmol) and 489 mg of $[Cp^*Ru(CH_3CN)_3]O_3SCF_3$ (0.96 mmol) in THF (20 ml) was refluxed for 30 min then allowed to cool to room temperature. Diethyl ether (40 ml) was added, precipitating a yellow powder. This was filtered off, washed with ether, and chromatographed on short column of activated neutral alumina (Merck 90) with acetone–ether (50:50) as eluant. Crystallization was achieved by allowing ether to diffuse slowly into the solution. Yield: 407 mg (93%). Analysis: found C, 48.00; H, 4.15. $Ru_2C_{40}H_{42}S_2O_6F_6$ (999.0 g/mol) calc.: C, 48.09; H, 4.24%.

$[(Cp^*Ru^I)(Cp^*Ru^{II})\eta^6,\eta^6$-chrysene$]O_3SCF_3$, 2. A solution of 77 mg of sodium naphthalene (0.51 mmol) in THF (0.348 mol/l) was added from a syringe to a vigorously stirred suspension of 509 mg of **1** (0.51 mmol) in dimethoxyethane in a Schlenk tube. The yellow suspension rapidly turned violet-blue, and finally a black solution and a white precipitate of NaO_3SCF_3 were formed. The latter was filtered off. The solution, which is stable but extremely sensitive towards oxygen, was evaporated *in vacuo* to yield **2**, which was washed with pentane and dried. Yield: 303 mg (70%). Analysis: found C, 55.05; H, 5.01. $Ru_2C_{39}H_{42}SO_3F_3$ (850.0 g/mol) calc.: C, 55.11; H, 4.98%.

Acknowledgments

We thank the FONDECYT Chile (Grants 624-89, 90-0012, 90-0013), the DAAD (Germany) and the Fonds der Chemischen Industrie (Germany) for support, Dr. E. Samuel (ENSC, Paris) for providing the ESR data, and Prof. P. Dixneuf (University of Rennes I) for providing the NMR data and for valuable discussions.

References

1 I. Chávez, A. Cisterna, M. Otero, E. Román and U. Müller, Z. Naturforsch., Teil B, 45 (1990) 658.

2 (a) D.O. Cowan, C. Levanda, J. Park and F. Kaufmann, Acc. Chem. Res., 6 (1973) 1; (b) D.N. Hendrickson, S.M. Oh and F.M. Moore, Comments Inorg. Chem., 4 (1985) 329; (c) U.T. Mueller-Westerhoff, Angew. Chem., Int. Ed. Engl., 25 (1986) 702; (d) N.G. Connelly and W.E. Geiger, Adv. Organomet. Chem., 23 (1984) 1.

3 (a) D. Astruc, Chem. Rev. 88 (1988) 1189; (b) D. Astruc, M.-H. Desbois, M. Lacoste, F. Moulines, J.-R. Hamon and F. Varret, Polyhedron, 9 (1990) 2727; (c) M. Lacoste, H. Rabaa, D. Astruc, N. Ardoin, F. Varret, J.-Y. Saillard and A. Le Beuze, J. Am. Chem. Soc., 112 (1990) 9548.

4 (a) P.J. Fagan, M.A. Ward and J.C. Calabrese, J. Chem. Soc., 111 (1989) 1689; (b) M.A. Ward, P.J. Fagan, J.C. Calabrese and D.C. Johnson, J. Am. Chem. Soc., 111 (1989) 1719; (c) U. Koelle and M.H. Wang, Organometallics, 9 (1990) 195.

5 (a) F.L. Carter, Molecular Electronic Devices, Marcel Dekker, New York, 1982; (b) F.L. Carter, Molecular Electronic Devices II, Marcel Dekker, New York, 1987; (c) K.V. Mikkelsen and M.A. Ratner, Chem. Rev., 87 (1987) 113; (d) K. Bange and T. Gambke, Adv. Mater., 64 (1990) 10.

6 (a) R.G. Sutherland, S.C. Chen, W.J. Pannekoek and C.C. Lee, J. Organomet. Chem., 117 (1976) 61; (b) C.C. Lee, K.J. Demchuk, W.J. Pannekoek and R.G. Sutherland, J. Organomet. Chem., 162 (1978) 253; (c) C.C. Lee, K.J. Demchuk and R.G. Sutherland, Can. J. Chem., 57 (1979) 933.

7 (a) A.M. McNair and K.R. Mann, Inorg. Chem., 25 (1986) 2519; (b) R.S. Koefod and K.R. Mann, J. Am. Chem. Soc., 112 (1990) 7287.

8 E. Samuel, E. Román and M. Otero, in preparation.

9 (a) K.D. Plitzko, B. Rapko, B. Gollas, G. Wehrle, T. Weakley, D.T. Pierce, W. Geiger Jr, R.C. Haddon and V. Boekelheide, J. Am. Chem. Soc., 112 (1990) 6545; (b) K.D. Plitzko, G. Wehrle, B. Gollas, B. Rapko, J. Daunheim and V. Boekelheide, J. Am. Chem. Soc., 112 (1990) 6556.

10 H.M. Koepp, H. Wendt and H. Strehlow, Z. Electrochem., 64 (1960) 83.

11 T.P. Angelicis and W.R. Heinemann, J. Chem. Ed., 53 (1976) 594.

12 D. Gourier and E. Samuel, J. Am. Chem. Soc., 109 (1987) 4571.

13 G.M. Sheldrick, SHELX-76, Program for the Determination of Crystal Structures. Univ. Cambridge, England, 1976.

14 C.K. Johnson, ORTEP, Report ORNL-3794, Oak Ridge National Laboratory, Tennessee, 1965.

15 (a) D.T. Cromer and J.B. Mann, Acta Crystallogr., Sect. A, 24 (1968) 321; (b) D.T. Cromer and D. Liberman, J. Chem. Phys., 53 (1970) 1891.

16 W.C. Hamilton, Acta Crystallogr., 12 (1959) 609.